Int. J. Nano Dimens., 14 (2): 167-177, Spring 2023

ORIGINAL ARTICLE

Using spray dried nanofibrillated Cellulose as an alternative to upgrading its effect in PLA nanocomposite

Somayeh Ghasemi[1], Rabi Behrooz[1,*], Maryam Rahimi [2]

[1] Department of Wood and Paper Science and Technology, Faculty of Natural Resources and Marine Sciences, Tarbiat Modares University, Iran
[2] Technical consultant, Technology and Innovation Center, Australia

Received 31 December 2022, revised 14 February 2023, accepted 20 February 2023, available 28 February 2023

Abstract

This research used an oven and sprays drying method to dry nanofibrillated cellulose (NFC) and evaluates its effect on polylactic acid (PLA) nanocomposite properties. As shown by atomic force microscopy (AFM), the average size of nanocellulose in the spray-dried sample (NCSD) was 84-96 nm. However, the average size of nanocellulose obtained from oven drying was 647-697 µm. The average size of the NCSD sample indicates that spray drying kept nanocellulose in the nano-scale range after drying. A melting process was then used to reinforce the polylactic acid matrix with the spray and oven-dried nanocellulose. Compared to neat PLA and PLA-containing oven-dried forms of nanocellulose (PLA-NCOD), our results showed a significant improvement in the mechanical strength of nanocomposites containing PLA-NCSD. PLA-NCSD nanocomposite demonstrated greater thermal stability than neat PLA and PLA-NCOD when subjected to thermal analysis. This study clearly illustrates the comparative effect of spray-dried nanocellulose on reinforced nanocellulose/PLA composites.

Keywords: *Mechanical Properties; Nanocellulose Drying; Nanofibrillated Cellulose (NFC); Polylactic Acid; Thermal Properties.*

How to cite this article

Ghasemi S., Behrooz R., Rahimi M. Using spray dried nanofibrillated Cellulose as an alternative to upgrading its effect in PLA nanocomposite. Int. J. Nano Dimens., 2023; 14(2): 167-177.

INTRODUCTION

There has been much interest in cellulose, which is an abundant polymer in nature, as an alternative source of nanosized reinforcement for many applications, including papermaking, high-quality nanocomposites, and medical products [1, 2] . Thus, it has the potential to be the most abundant and renewable natural resource in the world [3-5].

Even though polylactic acid (PLA) is a biodegradable biomass material, its brittleness, low flexibility, and other mechanical properties result in its limited use in engineering applications [6-8]. Nanocellulose has been shown to enhance the mechanical properties of biomass materials [2, 9, 10]. Nanocellulose consists of groups of cellulose chains that are bonded together by hydrogen bonds [1, 10]. It is important to note that they have different extraction procedures and morphologies [2, 3, 11]. Woody/non-woody, tunicates, algae, and bacteria can produce cellulose nanomaterials (CNMs) [12, 13]. Because the synthesis of these sources differs, subsequent CNMs have a variety of crystallinity, aspect ratios, and morphologies [12, 14].

As a result of the extraction process, CNMs may have different morphologies and surface chemistry depending on whether they are extracted mechanically, by acidic hydrolysis, or by a combination of these methods [15]. It has been determined that the cellulose nanofibers

* Corresponding Author Email: *rabi.behrooz@modares.ac.ir*

(CNFs) and the cellulose nanocrystals (CNCs) are the two primary structures of CNMs derived from these treatments. Acidic hydrolysis extraction produces large amount of waste acidic liquid after the extraction process, presenting environmental hazards and requiring repeated centrifuge and dialysis procedures. This method is also time-consuming [16-18]. Refining and homogenizing [19-21], microfluidization [22-24], grinding [25-27], cryocrushing [26], and high-intensity ultrasonication [28-30] are several mechanical methods for reducing cellulosic fibers to nanofibers. It is noteworthy that CNMs possess a high aspect ratio, Young's modulus of 114 GPa, and tensile strength of 6000 MPa, all of which are remarkably similar to those of the conventional inorganic fillers, which, however, are not biodegradable [2, 14]. Nanocellulose is typically produced in aqueous suspension due to its polar state [31, 32]. Since the majority of polymers are hydrophobic, in order to produce composite materials, water must be removed before mixing nanocellulose and polymers [32, 33]. It is highly desirable to apply dried nanocellulose into composites; hence, numerous research and development efforts have been conducted to develop methods of delivering dried nanocellulose for this purpose [33-36].

It has been found that water limits the efficacy of thermal compounding processes when using non-polar thermoplastics [37]. Consequently, in order to develop industrially relevant polymer nanocomposites, it is necessary to dry and understand the drying process for aqueous suspensions of nanocellulose. Furthermore, drying decreases the cost of transporting nanocellulose suspensions containing a high water content [32, 35]. With the advent of producing nanocellulose in large scale, new applications in the plastics industry are possible, such as the use of nanocellulose for reinforcing polymers [32]. It is, therefore, essential to dry nanocellulose suspensions. Different kinds of drying processes have been developed for CNMs, including solvent evaporation [35], Lyophilization [38, 39], supercritical fluids [40], and spray drying [41, 42].

CNMs tend to agglomerate in dry form, as outlined above. Therefore, drying nanocellulose in such a way that their size stays within nanometres is an important challenge for the industry. Incorporating spray-dried nanocellulose into nanocomposites has been subjected to limited research. In this study, we aim to use two different industrial and cost-effective nanocellulose drying methods to study the effect of these drying methods on the morphology, thermal properties, and mechanical properties of nanocomposites.

EXPERIMENTAL

Materials and the synthesis methods

A linter-dissolving pulp with cellulose content exceeding 95% and a polymerization degree (DP) of nearly 1800 was supplied by Linter Pak Co. in Behshahr, Iran. Due to hydrogen bonds that can be regenerated between CNFs upon drying[43], the pulp was never dried (30% consistency), facilitating microfibrillation and nanofibrillation. We used deionized water throughout the experiment, as well as no chemical reagents in the experiment.

CNFs Extraction

Our first step was to cut the fibers into small pieces with scissors, then soak the pulp in deionized water for two hours before disintegrating it with a disintegrator. We refined fibers using the PFI mill refiner as a pretreatment. Following refinement, the pulp consistency of the refiner was 24%, and the rotation speed was 10,000 rpm respectively. A suspension with 2 wt% concentration was obtained by adding deionized water to the refined pulp dispersion. Afterward, the mixture was homogenized using a high-pressure homogenizer (SRH-60, China) with a pressure of 400 bar for ten cycles.

CNFs Drying Methods

To achieve a final weight concentration of 1 wt% before drying, dried cellulose nanofibrillated suspensions were mixed with distilled water for 4 minutes at 2000 rpm using Speed Mixer. Two drying methods (oven and spray drying) were used for cellulose nanofibrillated suspensions of 1 wt% consistency.

Oven-Drying (OD)

We placed CNFs suspensions in an oven set to 105 °C for 24 hours. After drying, the dried nanocellulose was milled to obtain better fines.

Spray-Drying (SD)

A Buchi Mini Spray Dryer B-290 laboratory spray dryer (Swiss) was employed to dry the suspension of CNFs. A high-purity nitrogen gas was used as the injected gas to create suspension droplets. The samples were dried at 180 °C in an inlet

temperature, 540 l/h, 4.5 ml/min pump rate, 35 m^3/h drying gas flow, and 90 °C outlet temperature of the spray dryer measured for the CNFs. After drying, all the CNFs were stored in plastic bags and desiccators at ambient temperature for future use.

Nanocomposites Production

Coperion Brabender (TSE 20, Duisburg, Germany) twin screw extruders were used to manufacture nanocomposites. They were processed in two steps: the master batch and the final extrusion in the extruder. Initially, oven/spray-dried CNFs and PLA were added in a dry state, mixed with PLA with a screw speed of 100 rpm, and the temperature profile varied from 160 °C in the feed zone to 185°C in the die. As a next step, the masterbatches were diluted with fresh PLA to reach the final composition. The formulations of the prepared materials are shown in Table 1. In accordance with ASTM D638 type 5, the extruded pellets were dried at 55 °C for 6 hours before being injected molded (Haake MiniJet II) into test specimens. The injection molding machine barrel temperature was set at 190 °C. Injection-molded specimens were used to evaluate mechanical properties and thermal properties.

Characterization Techniques

In order to prepare the samples, linter and refined pulp suspensions were diluted to 0.5 weight percent, then placed on glass slides and stamped with coverslips. An optical microscope (Leica DMLM) was used to observe the fibers, while a digital imaging system measured their diameter. In this study, an Easyscan 2 Flex AFM probe microscope was used to analyze the morphology of suspensions and dried forms of CNFs. We prepared the samples by dispersing 1 mg of nanofibers in distilled water in an ultrasonic bath for 30 minutes, cast them onto a microscopy slide, and dried them in a vacuum oven at 70 °C for 1 hour.

Scanning Electron Microscopy (SEM) was used to investigate nanocomposites. Cryofracture surfaces were analyzed using Hitachi S-4700 (Schaumburg, IL, USA). To avoid charging, samples were coated with carbon sputtering. In order to determine the thermal stability of dried CNFs, a thermo-gravimetric analyzer (PL-TGA, Polymer Laboratories, England) was used to heat samples under a nitrogen atmosphere from 25 °C to 500 °C at a rate of 10 °C per minute. Tests of heat distortion temperature were conducted according to ASTM standard D648 using rectangular samples with dimensions of 127 x 12.7 x 3 mm under a load of 0.455 MPa and a heating rate of 2 °C/min.

Injection-molded specimens (ASTM D638 type 5) were used for the tensile test, and the gauge length was 30 mm. Tensile tests were performed using Hounsfield H25KS (United Kingdom) with a load cell of 10 kN. Each material was tested in five samples, and the average values were presented.

Using ASTM D256, we evaluated the unnotched Izod impact strength of PLA/nanocellulose composites and neat PLA, cutting rectangular bars 64 × 12.7 × 3 mm^3 from injection-molded sheets. At least five samples of each material were tested.

RESULTS AND DISCUSSION

Optical Microscopy (OM)

With the use of the PFI mill, the fibers became significantly looser, with many thin fibrils forming on their surface as a result of the refining treatment [19, 44]. It is impossible to extract long and high-purity CNFs through simple one-step chemical or mechanical methods, due to the strong hydrogen bonds between CNFs [45]. Consequently, it is essential that cotton fibers undergo refinement prior to nanofibrillation by the homogenizer (the second stage) [45, 46]. In the both linter dissolving pulp and refined pulp, cellulosic fibers were observed by optical microscopy (Fig. 1). According to Figure 1a, linter pulp had a length and width of 1.3 mm and 13 µm, respectively. This size was large for use in the high-pressure homogenizer directly. After refining, the length and width decreased to between 750 µm and 8µm, respectively, which allows it to be used directly in the high-pressure homogenizer (Fig. 1b).

Table 1. Nancellulose and PLA weight ratio in producing masterbatch and nanocomposite.

Sample	Masterbatch		Bulk PLA(g)
	CNFs (g)	PLA (g)	
PLA neat	-	-	100
PLA/spray dried nanocellulose (PLA-NCSD)	5	15	80
PLA/Oven dried nanocellulose (PLA-NCOD)	5	15	80

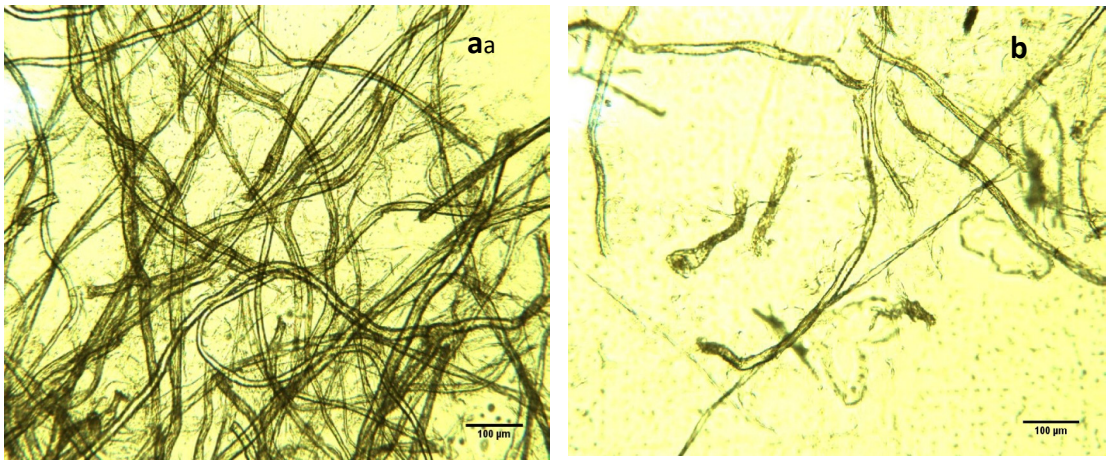

Fig. 1. Fibre morphology of linter dissolving before (a) and after refining (b).

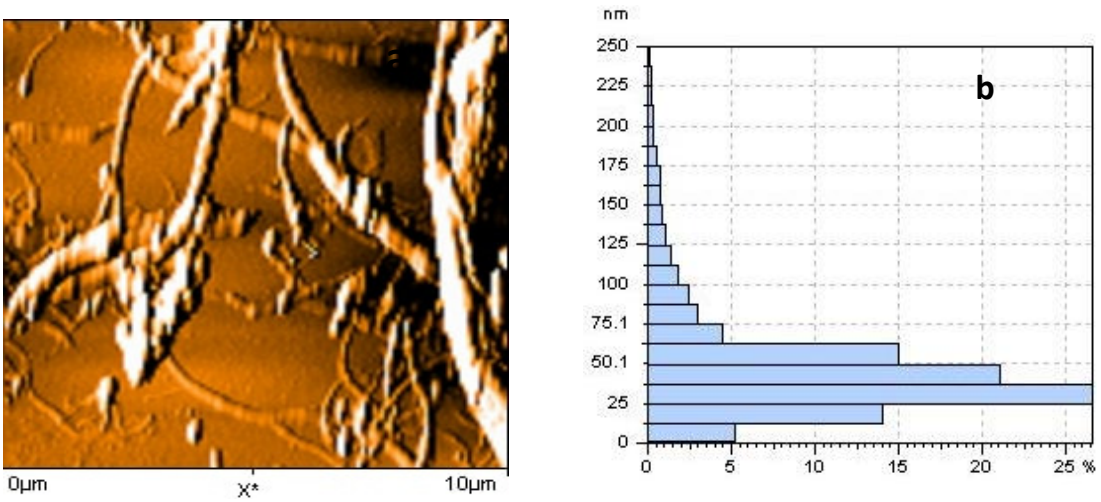

Fig. 2. AFM image (a) and size distribution of CNFs before drying (b).

Morphology Observation by AFM

In this study, using an AFM, nanofibrillated cellulose (NFCs) was observed on a nanoscale. The AFM images of nanofibrillated cellulose (NFCs) prepared by a high-pressure homogenizer are shown in Fig. 2a, and a size distribution diagram is shown in Fig. 2b. According to research, the average size of the CNFs produced by the homogenizer was approximately 25-37.5 nm. CNFs vary in morphology and properties according to their source of raw material and extraction process [47]. In research on cotton fibers treated with ionic liquid and then homogenized by high pressure, nanocellulose particles had diameters ranging from 10 to 30 nanometers. According to Fig. 3a, 3b, 3c, and 3d, drying methods affect both the morphology and size distribution of dried CNFs measured by AFM. Spray-dried CNFs have an average dimension of 84-96 nm and retain their nano-size dimensions. As a comparison, the drying of CNFs suspension in the oven (Fig. 3b) results in agglomeration and alteration in size. Several researchers have shown that conventional drying of nanocellulose at high temperatures through the evaporation of water can lead to agglomerated fiber due to hydrogen bonding between cellulose fibers [34, 35]. The nanometric scale of nanofibers is therefore lost with oven-dried CNFs. The average dimensions of oven-dried CNFs ranged from 647 to 700 nm. Powdery products containing nanoscale dimensions can be produced by spray drying CNF suspensions. As a consequence of spray drying,

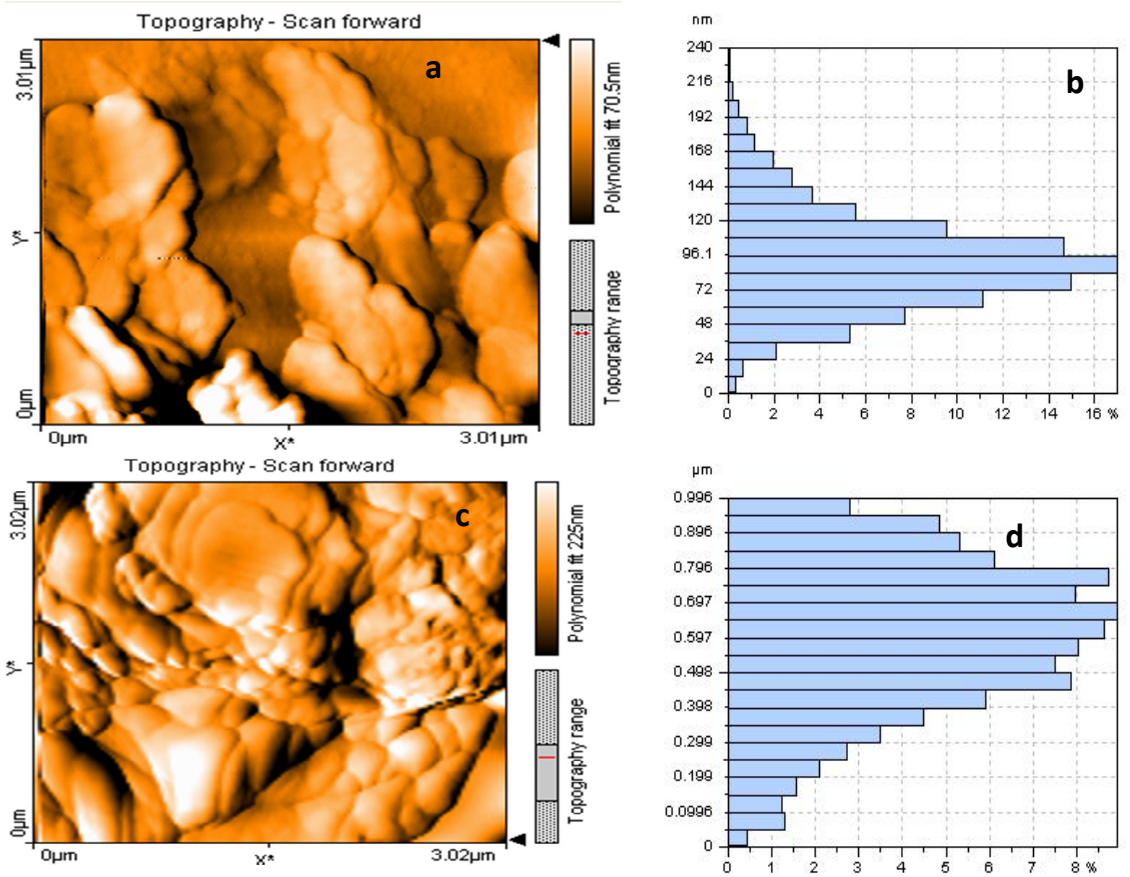

Fig. 3. AFM image and size distribution of spray-dried (NCSD) (a, b) and oven-dried (NCOD) (c, d) of CNFs.

particles are formed with various morphologies according to the source of nanocellulose [41, 42]. Park et al. investigated the morphology of spray-dried NFCs from bleached kraft pulps in 2017. Based on their measurements by AFM, the spray-dried CNFs showed a uniform fiber morphology with an average fiber size of 0.02-1000 µm [41]. In addition, other research has indicated that spray drying may be a viable method for drying nanoparticles that is both economical and desirable [32, 34, 41, 42].

SEM of the fracture surface of nanocomposites

The fracture cross-sectional SEM images in Figs. 4a, 4b, and 4c have been showed PLA, PLA-NCSD, and PLA-NCOD nanocomposites. Pure PLA has smooth surfaces and is brittle (Fig. 4a). Based on other research work [25], the fracture surface becomes uneven with nanocellulose incorporated into the PLA matrix due to the interfacial adhesive force [48, 49]. It is evident from Fig. 4c that the fracture surface of the composite with oven-dried nanocellulose has many holes and gaps, suggesting poor dispersion and weak interfacial bonding between the PLA matrix and the oven-dried nanocellulose. Compared to the oven-dried version, spray-dried nanocellulose is dispersed more uniformly in the matrix of the PLA-NCSD film due to fewer agglomerates (Fig. 4b). Many studies have observed these behaviours associated with the self-aggregation of nanocellulose due to hydrogen bonds between nanoparticles and incompatibility between hydrophilic CNC and hydrophobic matrix [25, 50-53].

Among other findings, Li *et al.* found large MFC agglomerates on the fracture surfaces of oven-dried MFC-PLA nanocomposite films [48]. According to them, these agglomerates may result in lower dispersibility in polymeric matrixes, as they act as defects/stress concentration points resulting in deterioration of composite properties.

Additionally, a study by Wei *et al.* examined

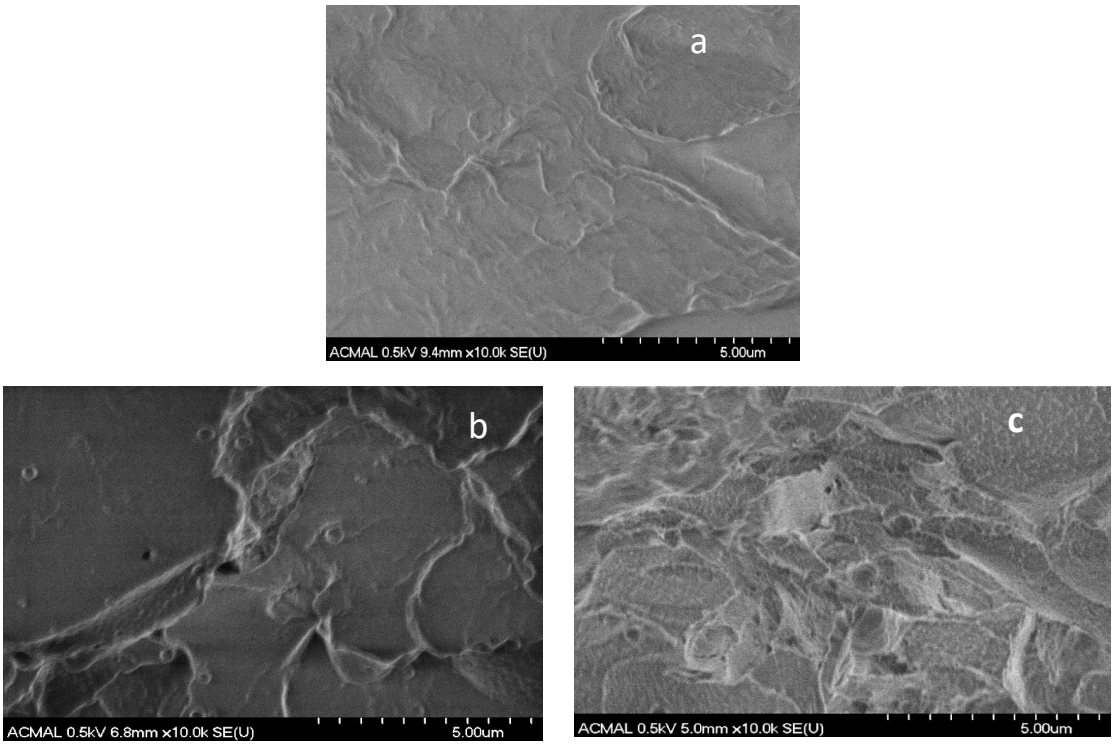

Fig. 4. SEM images of cryo-fractured surfaces of neat PLA (a) and PLA reinforced with 5% SD and OD CNF (b & c).

the fracture surfaces of freeze-dried CNCs and PLA by SEM [54]. The image revealed discontinuous zones and cavities within this nanocomposite film. According to them, these cavities result from large agglomerates/aggregates of freeze-dried CNCs as well as poor bonding at the interface.

TGA Analysis

As illustrated in Fig. 5, thermogravimetric analysis of the nanocomposites was conducted to examine their thermal degradation behaviors. Table 2 presents the thermal degradation data of neat PLA, PLA-NCSD, and PLA-NCOD nanocomposites at the temperatures at which 5% and 50% weight loss occurred, and residual weight at 500 °C was used. At 236.23 °C, 277.69 °C, and 6.94%, respectively, neat PLA shows T5, T50, and residual weight. With the incorporation of spray-dried nanocellulose, PLA thermal degradation temperatures increased from 23 °C to 30 °C, respectively. Nevertheless, the thermal degradation temperature was improved by 8.6 °C in the oven-dried form of nanocellulose compared to neat PLA. As a result of the incorporation of nanocellulose in PLA matrixes, the thermal stability was enhanced, and the thermal degradation was slowed down [55-57].

However, the spray-dried form of nanocellulose enhanced the thermal stability of the nanocomposite more than the incorporated oven-dried nanocellulose. This improvement is due to the intermolecular bonding between nanocellulose and polymers. In the study by Gan *et al.* the dispersion level of nanocellulose and the final morphology of the nanocomposites were significant factors in the enhancement of the thermal stability of the nanocomposite [57]. Therefore, the improved thermal stability of PLA-NCSD nanocomposites is associated with well-dispersed nanocellulose and effective interfacial adhesion between nanocellulose and polymer matrix. The thermal stability of nanocomposites may be affected by differences in sources of nanocellulose, matrix types, processing techniques, and drying processes [57].

Heat distortion temperature

As shown in Table 3, PLA has a low heat distortion temperature (HDT), making it unsuitable for use at high temperatures. As a result of spray-

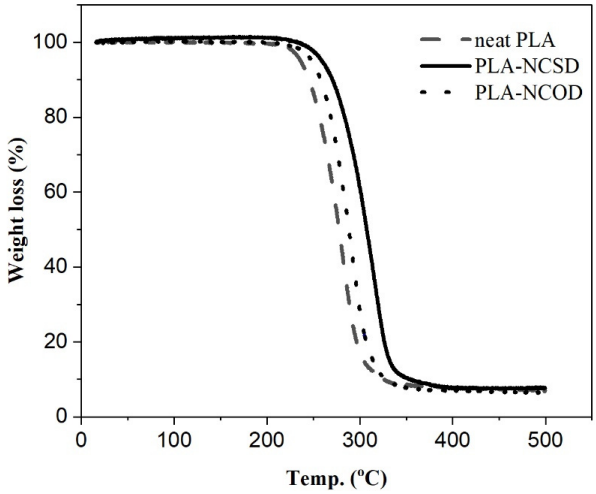

Fig. 5. TGA curve of neat PLA, PLA-NCSD, and PLA-NCOD bionanocomposites.

Table 2. Thermal degradation parameters of neat PLA, PLA-NCSD, and PLA-NCOD nanocomposites.

Sample	T_5 (°C)	T_{50} (°C)	Residual (%) at 500° C
Neat PLA	236.23	277.69	6.94
PLA-NCSD	259.61	307.26	7.68
PLA-NCOD	246.69	286.5	6.7

Table 3. Heat Distortion Temperature (HDT) of nanocellulose/PLA composite.

Treatment	**HDT (°C)**
Neat PLA	52.3±0.4
PLA/CNF 5(SD)	55.5±0.3
PLA/CNF5(OD)	51.1±1.2

dried nanocellulose addition to neat PLA, HDT increased slightly by 6.1% from 52.3 °C to 55.5 °C. Compared to PLA-NCOD nanocomposite, spray-dried CNFs/PLA nanocomposite increased HDT by 8.5%. There is evidence in several studies that adding cellulosic fiber increases the heat stability of PLA composite [58, 59]. In their study, Spinella *et al.* reported an improved HDT of PLA/CNF composites as a result of the effective dispersion of nanocellulose in the PLA [58].

Furthermore, according to Ding *et al.* [60], HDT changes are related to the composite preparation method, which affects the quality of dispersion and distribution of the nanocellulose in Polymeric matrix.

Mechanical properties

According to Fig. 6, the prepared nanocomposite demonstrated significant improvements in strength (Figure 6a), elongation at break (Figure 6b), and tensile modulus (Figure 6c) when compared to PLA-NCOD and neat PLA. The addition of 5% NCSD improved the tensile strength of PLA samples from 22.4 to 37.4 MPa, the elongation at break from 2.3 to 2.6%, and the tensile modulus from 1.1 to 1.7 GPa. Several research studies have attributed these improvements in tensile strength and modulus to the high mechanical properties of nanocellulose compared to the matrix [6, 49, 60].

Compared to neat PLA, PLA-NCOD composites had higher tensile strength and modulus, while their elongation at break decreased from 2.3 to 1.7%. Several factors influence the elongation at break, including the volume fraction of the added reinforcement, dispersion within the matrix, and interaction between reinforcement and matrix [61].

Li *et al.*, also observed a decrease in

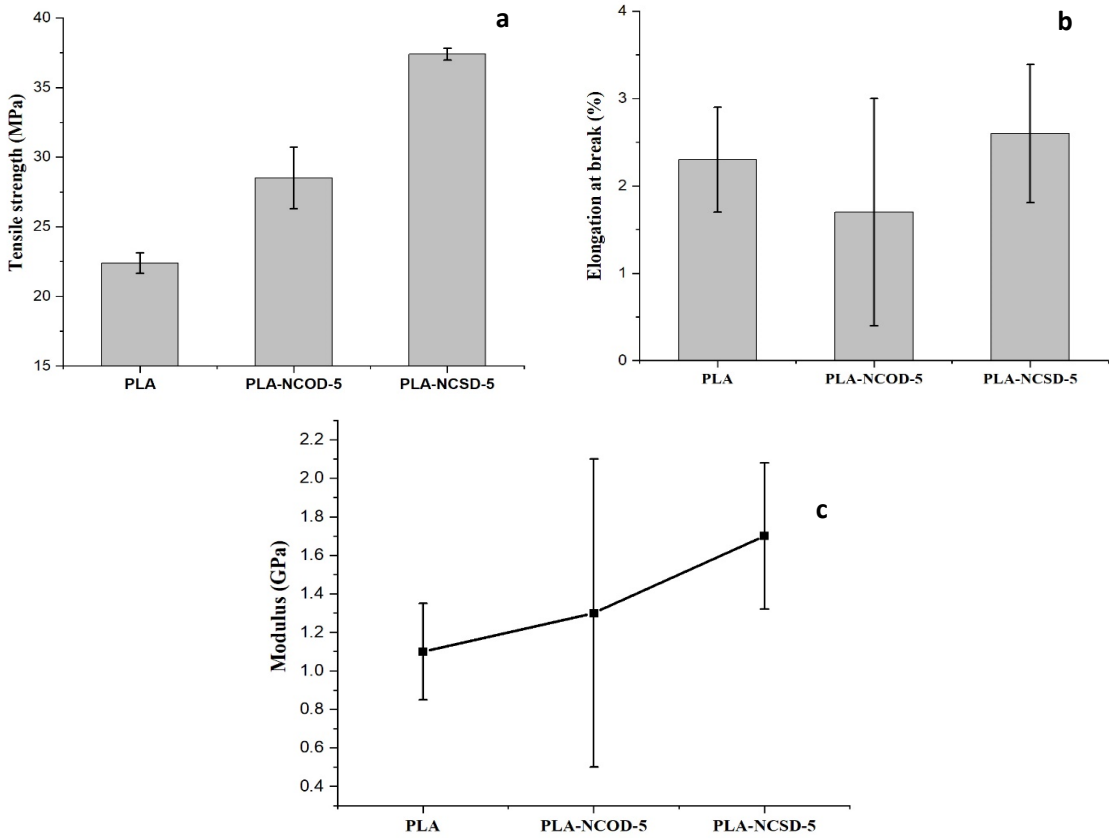

Fig. 6. Tensile strength (a), elongation at break (b) , and tensile modulus (c) for PLA, PLANFCOD-5, and PLANFCSD-5.

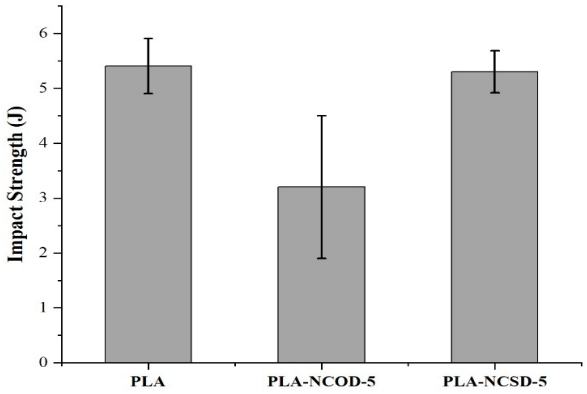

Fig. 7. Impact strength for PLA, PLANFCOD-5, and PLANFCSD-5.

elongation at the break of PLA/oven-dried NFCs nanocomposite compared to neat PLA [48]. Based on their findings, MFC agglomeration, lower dispensability, and the incompatibility between the hydrophilic MFC and hydrophobic PLA matrix might be involved in this issue.

Also, in comparison with neat PLA and PLA-NCOD nanocomposite, the spray-dried form of CNFs demonstrated greater elongation at the break by 13% and 53%, respectively. NFC has a high tensile modulus and strength because of its stiffness and potential adhesion between it and

the polymeric matrix [62].

A further explanation for the lower tensile parameters for PLA-NCOD nanocomposites is the agglomeration phenomena, which leads to weak fiber dispersion within the PLA matrix. In PLA-NCOD nanocomposite, the agglomeration of nanocellulose in the matrix may explain the reduction of elongation at break [63, 64]. Based on the findings of other researchers [6, 59, 65], nanosized cellulose may undergo microagglomeration. Based on Li *et al.*, MFC oven-dried particles act as defects/stress concentration points that result in poor stress transfer across the interphase and poor adhesion between the matrix and fibers, thereby causing a lack of strength improvement [48].

The lowest strength parameters were reported in a study by Peric *et al.* on freeze-dried NFC/PLA composites [38]. They concluded that the lack of improvement in tensile strength indicates the poor stress transfer across the interphase, so there is no interfacial bonding between the reinforcing fiber and the polymer matrix [38].

Impact strength

Fig. 7 illustrates the unnotch impact strength of PLA according to Izod. Pure PLA has impact strength of 5.4 J. The pure PLA had impact strength of 5.4 J. In the presence of oven-dried nanocellulose content, the impact strength of the nanocomposite decreased to 3.2 J. When oven-dried CNFs are incorporated into a polymeric matrix, impact strength has been reduced by 53% compared to neat PLA. PLA-NCSD nanocomposite did not show any significant improvement over neat PLA. However, PLA-NCSD nanocomposite demonstrated higher impact strength than PLA-NCOD nanocomposite.

In a study conducted by Peric *et al.*, which supports our findings, modified freeze-dried NFC added to PLA matrix did not improve impact strength. Also, unmodified MFC added to PLA matrix decreased the impact strength of the composite [38].

Figure 7 also illustrates how PLA-NCOD nanocomposites exhibit a higher variance in impact strength results due to a weak connection to the polymer matrix [66]. Other researchers have suggested that the low impact strength of PLA-NCOD could be attributed to the poor dispersion of nanocellulose in a polymeric matrix and the weak connection between them [67-69]. Other researchers also observed these characteristics and inferred that nanocellulose had poor dispersion or insufficient dispersibility, which inhibited the transfer of the load between two phases [39, 49].

CONCLUSIONS

In this study, CNFs are extracted from linter-dissolving pulp using a high-pressure homogenizer. AFM analysis of dried CNFs suggests that spray drying preserves their nano-scale dimensions. When spray and oven-dried CNFs were applied to the PLA matrix, PLA-NCSD nanocomposites were found to demonstrated higher tensile modulus, strength, and elongation than neat PLA and PLA-NCOD nanocomposites.

Based on SEM morphology studies of PLA and its nanocomposites, PLA-NCSD nanocomposite fracture surfaces were relatively smooth. Additionally, the HDT results indicated that the PLA-NCSD nanocomposite had a higher value than the PLA-NCOD nanocomposite based on the HDT results. Compared with oven-dried CNF/PLA nanocomposite, neat PLA has higher impact strength. When compared to neat PLA, spray-dried CNF/PLA nanocomposites did not significantly improve impact strength.

DECLARATION STATEMENT

The authors declare that they have no conflict of interest.

REFERENCES

1. Mishra R. K., Sabu A., Tiwari S. K., (2018), Materials chemistry and the futurist eco-friendly applications of nanocellulose: Status and prospect. *J. Saudi. Chem. Soc.* 22: 949-978.
2. Trache D., Tarchoun A. F., Derradji M., Hamidon T. S., Masruchin N., Brosse N., Hussin M. H., (2020), Nanocellulose: From fundamentals to advanced applications. *Front. Chem.* 8: 392-396.
3. Jonoobi M., Oladi R., Davoudpour Y., Oksman K., Dufresne A., Hamzeh Y., Davoodi R., (2015), Different preparation methods and properties of nanostructured cellulose from various natural resources and residues: A review. *Cellulose.* 22: 935-969.
4. Yeganeh F., Behrooz R., Rahimi M., (2017), The effect of Sulfuric acid and Maleic acid on characteristics of nano-cellulose produced from waste office paper. *Int. J. Nano Dimens.* 8: 206-215.
5. Dashtbani R., Afra E., (2015), Producing cellulose nanofiber from cotton wastes by electrospinning method. *Int. J. Nano Dimens.* 6: 1-9.
6. Huang L., Zhang X., Xu M., Chen J., Shi Y., Huang C., Wang S., An S., Li C., (2018), Preparation and mechanical properties of modified nanocellulose/PLA composites from cassava residue. *AIP Adv.* 8: 025116-025120.

7. Kumari S. V. G., Pakshirajan K., Pugazhenthi G., (2022), Recent advances and future prospects of cellulose, starch, chitosan, polylactic acid and polyhydroxyalkanoates for sustainable food packaging applications. *Int. J. Biol. Macromol.* 30: 163-182.
8. Taib N.-A. A. B., Rahman M. R., Huda D., Kuok K. K., Hamdan S., Bakri M. K. B., Julaihi M. R. M. B., Khan A., (2022), A review on poly lactic acid (PLA) as a biodegradable polymer. *Polym. Bull.* 2: 1-35.
9. Dhali K., Daver F., Cass P., Adhikari B., (2022), Surface modification of the cellulose nanocrystals through vinyl silane grafting. *Int. J. Biol. Macromol.* 200: 397-408.
10. Eichhorn S. J., Etale A., Wang J., Berglund L. A., Li Y., Cai Y., Chen C., Cranston E. D., Johns M. A., Fang Z., (2022), Current international research into cellulose as a functional nanomaterial for advanced applications. *J. Mater. Sci.* 57: 5697-5767.
11. Thakur V., Guleria A., Kumar S., Sharma S., Singh K., (2021), Recent advances in nanocellulose processing, functionalization and applications: A review. *Mater. Adv.* 2: 1872-1895.
12. Mokhena T., Sefadi J., Sadiku E., John M., Mochane M., Mtibe A., (2018), Thermoplastic processing of PLA/cellulose nanomaterials composites. *Polym.* 10: 1363-1367.
13. Norizan M. N., Shazleen S. S., Alias A. H., Sabaruddin F. A., Asyraf M. R. M., Zainudin E. S., Abdullah N., Samsudin M. S., Kamarudin S. H., Norrrahim M. N. F., (2022), Nanocellulose-based nanocomposites for sustainable applications: A review. *Nanomater.* 12: 3483-3487.
14. Foster E. J., Moon R. J., Agarwal U. P., Bortner M. J., Bras J., Camarero-Espinosa S., Chan K. J., Clift M. J., Cranston E. D., Eichhorn S. J., (2018), Current characterization methods for cellulose nanomaterials. *Chem. Soc. Rev.* 47: 2609-2679.
15. Scaffaro R., Botta L., Lopresti F., Maio A., Sutera F., (2017), Polysaccharide nanocrystals as fillers for PLA based nanocomposites. *Cellulose.* 24: 447-478.
16. Chen Y. W., Lee H. V., Abd Hamid S. B., (2017), Facile production of nanostructured cellulose from Elaeis guineensis empty fruit bunch via one pot oxidative-hydrolysis isolation approach. *Carbohydr. Polym.* 157: 1511-1524.
17. Pires J. R., Souza V. G., Fernando A. L., (2019), Valorization of energy crops as a source for nanocellulose production–current knowledge and future prospects. *Ind. Crops. Prod.* 140: 111642-111646.
18. Nagarajan K., Ramanujam N., Sanjay M., Siengchin S., Surya Rajan B., Sathick Basha K., Madhu P., Raghav G., (2021), A comprehensive review on cellulose nanocrystals and cellulose nanofibers: Pretreatment, preparation, and characterization. *Polym. Compos.* 42: 1588-1630.
19. Ang S., Haritos V., Batchelor W., (2019), Effect of refining and homogenization on nanocellulose fiber development, sheet strength and energy consumption. *Cellulose.* 26: 4767-4786.
20. Wang Y., Wei X., Li J., Wang F., Wang Q., Zhang Y., Kong L., (2017), Homogeneous isolation of nanocellulose from eucalyptus pulp by high pressure homogenization. *Ind. Crops. Prod.* 104: 237-241.
21. Lindström T., (2017), Aspects on nanofibrillated cellulose (NFC) processing, rheology and NFC-film properties. *Curr. Opin. Colloid Interf. Sci.* 29: 68-75.
22. Poyraz B., Tozluoğlu A., Candan Z., Demir A., (2017), Matrix impact on the mechanical, thermal and electrical properties of microfluidized nanofibrillated cellulose composites. *J. Polym. Eng.* 37: 921-931.
23. Campos A. D., Neto A. R., Rodrigues V. B., Kuana V. A., Correa A. C., Takahashi M. C., Mattoso L. H., Marconcini J. M., (2017), Production of cellulose nanowhiskers from oil palm mesocarp fibers by acid hydrolysis and microfluidization. *J. Nanosci. Nanotechnol.* 17: 4970-4976.
24. Rashid S., Dutta H., (2020), Characterization of nanocellulose extracted from short, medium and long grain rice husks. *Ind. Crops. Prod.* 154: 112627-112631.
25. Abdulkhani A., Hosseinzadeh J., Dadashi S., Mousavi M., (2015), A study of morphological, thermal, mechanical and barrier properties of PLA based biocomposites prepared with micro and nano sized cellulosic fibers. *Cellul. Chem. Technol.* 49: 597-605.
26. Supian M. A. F., Amin K. N. M., Jamari S. S., Mohamad S., (2020), Production of cellulose nanofiber (CNF) from empty fruit bunch (EFB) via mechanical method. *J. Environ. Chem. Eng.* 8: 103024-103027.
27. Gemmer R. E., Borsoi C., Hansen B., Dahlem Júnior M. A., Francisquetti E. L., Rossa Beltrami L. V., Zattera A. J., Catto A. L., (2021), Extraction of nanocellulose from yerba mate residues using steam explosion, TEMPO-mediated oxidation and ultra-fine friction grinding. *J. Nat. Fibers*. 19: 10539-10549.
28. Wang H., Zhang X., Jiang Z., Yu Z., Yu Y., (2016), Isolating nanocellulose fibrills from bamboo parenchymal cells with high intensity ultrasonication. *Holzforschung.* 70: 401-409.
29. Yang X., Han F., Xu C., Jiang S., Huang L., Liu, L., Xia Z., (2017), Effects of preparation methods on the morphology and properties of nanocellulose (NC) extracted from corn husk. *Ind. Crops. Prod.* 109: 241-247.
30. Das D., Das M. J., Muchahary S., Deka S. C., (2019), Nanocellulose-based paper from banana peduncle using high-intensity ultrasonication. *In Applied Food Science and Eng. with Ind. Applic.* (pp. 29-46): Apple Academic Press.
31. Phanthong P., Reubroycharoen P., Hao X., Xu G., Abudula A., Guan G., (2018), Nanocellulose: Extraction and application. *Carbon Resour. Convers.* 1: 32-43.
32. Sinquefield S., Ciesielski P. N., Li K., Gardner D. J., Ozcan S., (2020), Nanocellulose dewatering and drying: Current state and future perspectives. *ACS Sustainable Chem. Eng.* 8: 9601-9615.
33. Noguchi T., Niihara K.-i., Iwamoto R., Matsuda G.-i., Endo M., Isogai, A., (2021), Nanocellulose/polyethylene nanocomposite sheets prepared from an oven-dried nanocellulose by elastic kneading. *Compos. Sci. Technol.* 207: 108734-108737.
34. Zimmermann M. V., Borsoi C., Lavoratti A., Zanini M., Zattera A. J., Santana R. M., (2016), Drying techniques applied to cellulose nanofibers. *J. Reinf. Plast. Compos.* 35: 628-643.
35. Hanif Z., Jeon H., Tran T. H., Jegal J., Park S.-A., Kim S.-M., Park J., Hwang S. Y., Oh D. X., (2018), Butanol-mediated oven-drying of nanocellulose with enhanced dehydration rate and aqueous re-dispersion. *J. Polym. Res.* 25: 1-11.
36. Huang J., Dufresne A., Lin N., (2019), *Nanocellulose: From Fundamentals to Adv. Mater*: John Wiley & Sons.
37. Wang L., Sanders J. E., Gardner D. G., Han Y., (2016), In-situ modification of cellulose nanofibrils by organosilanes during spray drying. *Ind. Crops Prod.* 93: 129-135.
38. Perić M., Putz R., Paulik C., (2019), Influence of nanofibrillated cellulose on the mechanical and thermal

properties of poly (lactic acid). *Eur. Polym. J.* 114: 426-433.
39. He L., Song F., Li D.-F., Zhao X., Wang X.-L., Wang Y.-Z., (2020), Strong and tough polylactic acid based composites enabled by simultaneous reinforcement and interfacial compatibilization of microfibrillated cellulose. *ACS Sustain. Chem. Eng.* 8: 1573-1582.
40. Wang X., Zhang Y., Jiang H., Song Y., Zhou Z., Zhao H., (2016), Fabrication and characterization of nano-cellulose aerogels via supercritical CO_2 drying technology. *Mater. Lett.* 183: 179-182.
41. Park C.-W., Han S.-Y., Namgung H.-W., Seo P.-N., Lee S.-H., (2017), Effect of spray-drying condition and surfactant addition on morphological characteristics of spray-dried nanocellulose. *J. Environ. Sci.* 33: 33-38.
42. Furtado M. R., da Matta V. M., Carvalho C. W., Magalhães W. L., Rossi A. L., Tonon R. V., (2021), Characterization of spray-dried nanofibrillated cellulose and effect of different homogenization methods on the stability and rheological properties of the reconstituted suspension. *Cellulose.* 28: 207-221.
43. Zhao J., Zhang W., Zhang X., Zhang X., Lu C., Deng Y., (2013), Extraction of cellulose nanofibrils from dry softwood pulp using high shear homogenization. *Carbohyd. Polym.* 97: 695-702.
44. Oliaei E., Lindén P. A., Wu Q., Berthold F., Berglund L., Lindström T., (2020), Microfibrillated lignocellulose (MFLC) and nanopaper films from unbleached kraft softwood pulp. *Cellulose.* 27: 2325-2341.
45. Balea A., Blanco A., Delgado-Aguilar M., Monte M. C., Tarres Q., Mutjé P., Negro C., (2021), Nanocellulose characterization challenges. *Bioresources.* 16: 4382-4410.
46. Lee H., Mani S., (2017), Mechanical pretreatment of cellulose pulp to produce cellulose nanofibrils using a dry grinding method. *Ind. Crops. Prod.* 104: 179-187.
47. Kar K. K., Rana S., Pandey J., (2015), *Handbook of polymer nanocomposites processing, performance and application*: Springer.
48. Li K., Mcgrady D., Zhao X., Ker D., Tekinalp H., He X., Qu J., Aytug T., Cakmak E., Phipps J., (2021), Surface-modified and oven-dried microfibrillated cellulose reinforced biocomposites: Cellulose network enabled high performance. *Carbohyd. Polym.* 256: 117525-117529.
49. Tian J., Cao Z., Qian S., Xia Y., Zhang J., Kong Y., Sheng K., Zhang Y., Wan Y., Takahashi J., (2022), Improving tensile strength and impact toughness of plasticized poly (lactic acid) biocomposites by incorporating nanofibrillated cellulose. *Nanotechnol. Rev.* 11: 2469-2482.
50. Ansari F., Skrifvars M., Berglund L., (2015), Nanostructured biocomposites based on unsaturated polyester resin and a cellulose nanofiber network. *Compos. Sci. Technol.* 117: 298-306.
51. Nagalakshmaiah M., Mortha G., Dufresne A., (2016), Structural investigation of cellulose nanocrystals extracted from chili leftover and their reinforcement in cariflex-IR rubber latex. *Carbohydr. Polym.* 136: 945-954.
52. Li Y.-D., Fu Q.-Q., Wang M., Zeng J.-B., (2017), Morphology, crystallization and rheological behavior in poly (butylene succinate)/cellulose nanocrystal nanocomposites fabricated by solution coagulation. *Carbohydr. Polym.* 164: 75-82.
53. Sapkota J., Natterodt J. C., Shirole A., Foster E. J., Weder C., (2017), Fabrication and properties of polyethylene/cellulose nanocrystal composites. *Macromol. Mater. Eng.* 302: 1600300-1600304.
54. Wei L., Agarwal U. P., Hirth K. C., Matuana L. M., Sabo R. C., Stark N. M., (2017), Chemical modification of nanocellulose with canola oil fatty acid methyl ester. *Carbohydr. Polym.* 169: 108-116.
55. Mondragon G., Peña-Rodriguez C., González A., Eceiza A., Arbelaiz A., (2015), Bionanocomposites based on gelatin matrix and nanocellulose. *Eur. Polym. J.* 62: 1-9.
56. Khoo R., Ismail H., Chow W., (2016), Thermal and morphological properties of poly (lactic acid)/nanocellulose nanocomposites. *Procedia. Chem.* 19: 788-794.
57. Gan P., Sam S., Abdullah M. F. B., Omar M. F., (2020), Thermal properties of nanocellulose-reinforced composites: A review. *J. Appl. Polym. Sci.* 137: 48544-48548.
58. Spinella S., Re G. L., Liu B., Dorgan J., Habibi Y., Leclere P., Raquez J.-M., Dubois P., Gross R. A., (2015), Polylactide/cellulose nanocrystal nanocomposites: Efficient routes for nanofiber modification and effects of nanofiber chemistry on PLA reinforcement. *Polym.* 65: 9-17.
59. Ghasemi S., Behrooz R., Ghasemi I., Yassar R. S., Long F., (2018), Development of nanocellulose-reinforced PLA nanocomposite by using maleated PLA (PLA-g-MA). *J. Thermoplast. Compos. Mater.* 31: 1090-1101.
60. Ding W. D., Pervaiz M., Sain M., (2018), Cellulose-enabled polylactic acid (PLA) nanocomposites: Recent developments and emerging trends. *In Functional biopolym.* (pp. 183-216).
61. Shojaeiarani J., Bajwa D. S., Chanda S., (2021), Cellulose nanocrystal based composites: A review. *Compos. Part C: Open Access.* 5: 100164-100167.
62. Zaaba N. F., Jaafar M., Ismail H., (2021), Tensile and morphological properties of nanocrystalline cellulose and nanofibrillated cellulose reinforced PLA bionanocomposites: A review. *Polym. Eng. Sci.* 61: 22-38.
63. Yang W., Dominici F., Fortunati E., Kenny J. M., Puglia D., (2015), Melt free radical grafting of glycidyl methacrylate (GMA) onto fully biodegradable poly (lactic) acid films: Effect of cellulose nanocrystals and a masterbatch process. *RSC Adv.* 5: 32350-32357.
64. Gitari B., Chang B. P., Misra M., Navabi A., Mohanty A. K., (2019), A comparative study on the mechanical, thermal, and water barrier properties of PLA nanocomposite films prepared with bacterial nanocellulose and cellulose nanofibrils. *Bioresources.* 14: 1867-1889.
65. Perić M., Putz R., Paulik C., (2019), Influence of nanofibrillated cellulose on the mechanical and thermal properties of poly (lactic acid). *Eur. Polym. J.* 114: 426-433.
66. Immonen K., Lahtinen P., Pere J., (2017), Effects of surfactants on the preparation of nanocellulose-PLA composites. *Bioeng.* 4: 91-96.
67. Peng Y., Gardner D. J., Han Y., (2015), Characterization of mechanical and morphological properties of cellulose reinforced polyamide 6 composites. *Cellulose.* 22: 3199-3215.
68. Immonen K., Lahtinen P., Pere J., (2017), Effects of surfactants on the preparation of nanocellulose-PLA composites. *Bioengineering.* 4: 91-96.
69. Lu J., Sun C., Yang K., Wang K., Jiang Y., Tusiime R., Yang Y., Fan F., Sun Z., Liu Y., (2019), Properties of polylactic acid reinforced by hydroxyapatite modified nanocellulose. *Polymers.* 11: 1009-1012.